ISSN 1068-3356, Bulletin of the Lebedev Physics Institute, 2024, Vol. 51, No. 11, pp. 465–469. © Allerton Press, Inc., 2024.
Russian Text © The Author(s), 2024, published in Kratkie Soobshcheniya po Fizike, 2024, Vol. 51, No. 11, pp. 53–59.

Inelastic Cross Sections of Interaction of Relativistic Heavy Nuclei

A. V. Bagulya[a,*], V. M. Grichine[a], V. N. Ivanchenko[b], V. A. Ryabov[a], and S. N. Filimonov[b]

[a] *Lebedev Physical Institute, Russian Academy of Sciences, Moscow, 119991 Russia*

[b] *National Research Tomsk State University, Tomsk, 634050 Russia*

**e-mail: bagulyaav@lebedev.ru*

Received September 10, 2024; revised September 28, 2024; accepted October 1, 2024

Abstract—The Geant4 software package is used to calculate hadronic and electromagnetic inelastic cross sections of interactions of relativistic heavy nuclei as functions of the center-of-mass energy per nucleon. It is shown that in the energy range of the NICA accelerator complex, inelastic collisions result from electromagnetic dissociation of colliding nuclei.

Keywords: inelastic cross section, electromagnetic dissociation, relativistic nucleus

DOI: 10.3103/S1068335624601705

Studying collisions of heavy atomic nuclei at high energies is of fundamental interest for investigating processes in the early Universe. One of the tasks of the Nuclotron-based Ion Collider fAcility (NICA)—the recently launched Russian accelerator complex—is an experimental study of collisions of heavy atomic nuclei at center-of-mass energies per nucleon $\sqrt{S_{NN}} \simeq 5$–11 GeV [1]. At these energies, the integral cross section of electromagnetic dissociation becomes comparable to or larger than the inelastic hadronic cross section.

In this paper, use is made of the Geant4 software package [2–6] to calculate integral inelastic hadronic and electromagnetic cross sections of collisions of relativistic heavy nuclei for characteristic NICA energies.

To describe hadronic nucleus–nucleus cross sections, we follow the simplified Glauber model with the Gribov corrections for inelastic screening [7, 8]. The model provides a simple analytical form for the integral cross sections:

$$\sigma_{\text{tot}}^{A_pA_t} = 2\pi(R_p^2 + R_t^2)\ln\left[1 + \frac{A_pA_t\sigma_{\text{tot}}^{NN}}{2\pi(R_p^2 + R_t^2)}\right], \quad (1)$$

$$\sigma_{\text{in}}^{A_pA_t} = \pi(R_p^2 + R_t^2)\ln\left[1 + \frac{A_pA_t\sigma_{\text{tot}}^{NN}}{\pi(R_p^2 + R_t^2)}\right], \quad (2)$$

$$\sigma_{\text{prod}}^{A_pA_t} = \pi(R_p^2 + R_t^2)\ln\left[1 + \frac{A_pA_t\sigma_{\text{in}}^{NN}}{\pi(R_p^2 + R_t^2)}\right], \quad (3)$$

with the definitions

$$\sigma_{\text{el}}^{A_pA_t} = \sigma_{\text{tot}}^{A_pA_t} - \sigma_{\text{in}}^{A_pA_t}, \quad \sigma_{\text{qel}}^{A_pA_t} = \sigma_{\text{in}}^{A_pA_t} - \sigma_{\text{prod}}^{A_pA_t}, \quad (4)$$

where $\sigma_{\text{tot}}^{A_pA_t}$ and $\sigma_{\text{in}}^{A_pA_t}$ are the total and inelastic cross sections of the reaction; $\sigma_{\text{prod}}^{A_pA_t}$ is the cross section for the production of new hadrons; and $\sigma_{\text{el}}^{A_pA_t}$ and $\sigma_{\text{qel}}^{A_pA_t}$ are the elastic and inelastic cross sections, respectively. The atomic weights of the incident nucleus and the target nucleus are $A_p = Z_p + N_p$ and $A_t = Z_t + N_t$, respectively. The notations Z and N correspond to the number of protons and neutrons in the nuclei, and $\sigma_{\text{tot/in}}^{NN}$ are the total/inelastic nucleon–nucleon cross sections:

$$A_pA_t\sigma_{\text{tot}}^{NN} = Z_pZ_t\sigma_{\text{tot}}^{pp} + N_pN_t\sigma_{\text{tot}}^{nn} + (Z_pN_t + N_pZ_t)\sigma_{\text{tot}}^{pn}. \quad (5)$$

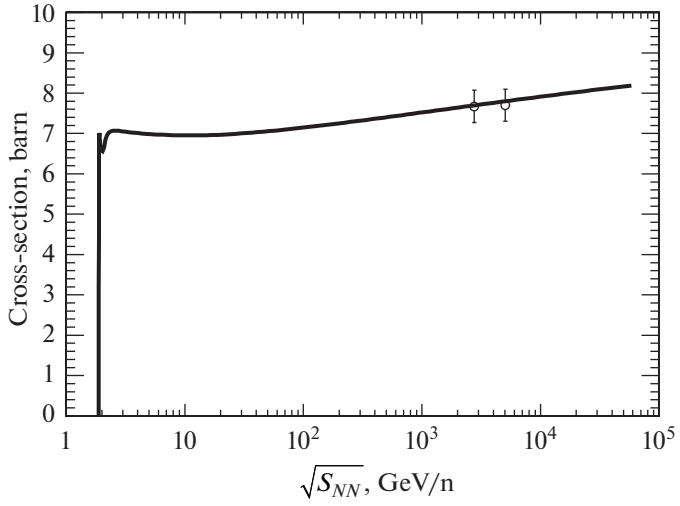

Fig. 1. Inelastic hadronic integral cross section for lead nucleus collisions as a function of the center-of-mass energy per nucleon. The curve is the calculation according to the Glauber–Gribov model. The dots are the experimental data [10].

Parameters R_p and R_t depend, respectively, on the atomic weights A_p and A_t [9]:

$$R(A) = \begin{cases} r_0(1 - A^{-2/3})A^{1/3}, & A < 50, \\ r_0 A^{0.27}, & A \geq 50, \end{cases} \tag{6}$$

where r_0 is the proton radius, equal to ~1 F.

At low energies, total and inelastic cross sections are corrected for the Coulomb barrier, B_c:

$$\sigma_{\text{tot/in}}^{A_pA_t} \to \sigma_{\text{tot/in}}^{A_pA_t}\left[1 - \frac{B_c}{T_{\text{kin}}^{cm}}\right], \quad B_c = \frac{Z_pZ_te^2}{R_{\min}}, \tag{7}$$

where T_{kin}^{cm} is the kinetic energy of the incident nucleus in the center-of-mass system, $R_{\min} \sim R_t + R_p$ and e is the electron charge.

The simplified Glauber–Gribov model predicts a weak relativistic increase in cross sections with increasing center-of-mass energy compared to nucleon cross sections. This prediction has been recently confirmed experimentally using the ALICE setup [10] (see Fig. 1).

The integral cross section of electromagnetic dissociation of a nucleus is expressed in the form [9]

$$\sigma_{ED} = N_{E1}(E_{GDR})\int\sigma_{E1}(E_\gamma)dE_\gamma + N_{E2}(E_{GQR})E_{GQR}^2\int\frac{\sigma_{E2}(E_\gamma)}{E_\gamma^2}dE_\gamma, \tag{8}$$

where the integrals of the dipole and quadrupole giant resonances can be approximately estimated as [11, 12]:

$$\int\sigma_{E1}(E_\gamma)dE_\gamma = 60\frac{N_pZ_p}{A_p}, \tag{9}$$

$$\int\sigma_{E2}(E_\gamma)\frac{dE_\gamma}{E_\gamma^2} = 0.22fZ_pA_p^{2/3}, \tag{10}$$

with $f = 0.9$ for heavy nuclei at $A_p > 100$. In relations (9) and (10), use is made of the measurement units of MeV mb and μb/MeV, respectively.

The energy dependence of the number of equivalent photons corresponding to the dipole field is given by [11]:

$$N_{E1}(E_\gamma) = \frac{2\alpha Z_t^2}{\pi\beta^2E_\gamma}\left\{\xi K_0(\xi)K_1(\xi) - \frac{\xi^2\beta^2}{2}\left(K_1^2(\xi) - K_0^2(\xi)\right)\right\}, \tag{11}$$

where α is the fine structure constant; β is the velocity of the incident nucleus in the laboratory frame of reference in units of the speed of light c in vacuum; γ is the Lorentz factor of the incident nucleus in the laboratory frame of reference; $\hbar$ is Planck's constant; E_γ is the energy of equivalent photons; and K_0 and K_1 are the modified Bessel functions of the second kind of the zeroth and first orders, respectively. Use is also made of parameters

$$\xi = \frac{E_\gamma b_{\min}}{\gamma\beta\hbar c}, \quad b_{\min} = (1 + x_d)b_c + \frac{\pi\alpha_0}{2\gamma},$$

$$\alpha_0 = \frac{Z_p Z_t e^2}{\mu\beta^2 c^2}, \quad b_c = 1.34\left[A_p^{1/3} + A_t^{1/3} - 0.75\left(A_p^{-1/3} + A_t^{-1/3}\right)\right],$$

where μ is the reduced mass of the incident nucleus and the target nucleus and $x_d = 0.25$ (b_c in F).

The energy dependence of the number of equivalent photons corresponding to the quadrupole field on the energy is given by

$$N_{E2}(E_\gamma) = \frac{2\alpha Z_t^2}{\pi\beta^4 E_\gamma}\left\{2(1-\beta^2)K_1^2(\xi) + \xi(2-\beta^2)^2 \times K_0(\xi)k_1(\xi) - \frac{\xi^2\beta^4}{2}\left(K_1^2(\xi) - K_0^2(\xi)\right)\right\}. \tag{12}$$

The energies of dipole and quadrupole resonances are, respectively, expressed in the form:

$$E_{GDR} = \hbar c\left[\frac{m^* c^2 R_0^2}{8J}\left(1 + u - \frac{1+\varepsilon+3u}{1+\varepsilon+u}\varepsilon\right)\right]^{-1/2}, \quad E_{GQR} = \frac{63}{A_p^{1/3}},$$

with parameters:

$$u = \frac{3J}{Q'}A_p^{-1/3}, \quad R_0 = r_0 A_p^{1/3},$$

where $\varepsilon = 0.0768$, $Q = 17$ MeV, $J = 36.8$ eV, $r_0 = 1.18$ F, $m^* = 0.7m_N$, and $m_N = 938.95$ MeV is the nucleon mass.

For heavy nuclei, the proton production cross section is

$$\sigma_{ED,p} = \sigma_{ED}\min\left[\frac{Z_p}{A_p}, 1.95\exp(-0.075Z_p)\right], \tag{13}$$

for $Z_p \geq 14$. The neutron production cross section is determined by the difference:

$$\sigma_{ED,n} = \sigma_{ED} - \sigma_{ED,p}.$$

Relation (8) is valid under the assumption of sharp peaks of the dipole and quadrupole resonances [11].

The simplified Glauber–Gribov model for nuclear collisions in the Geant4 software package is implemented in the *G4ComponentGGNuclNuclXsc* class, and the electromagnetic dissociation model is implemented in the *G4EMDissociationCrossSection* class. The nucleon cross sections are parameterized in the *G4HadronNucleonXsc* class.

Figure 2 shows the dependences of the inelastic collision cross sections of gold, lead, and uranium nuclei on the center-of-mass energy per nucleon. The solid curve illustrates inelastic hadron integral cross section according to the Glauber–Gribov model, and the dashed curve demonstrates the total cross section of electromagnetic dissociation. In the calculations we used relations (2) and (8) for the inelastic hadron cross section and the electromagnetic dissociation cross section, respectively.

The dependences of the inelastic cross sections of the nucleus–nucleus interaction on the center-of-mass energy per nucleon calculated using the Geant4 software package show that, for the characteristic energies of the NICA accelerator complex, the cross section of electromagnetic dissociation is several times greater than the hadronic inelastic integral cross section. The general reason (not only for nucleus–nucleus collisions) for the excess of the electromagnetic cross section over the hadronic cross section is a wider spatial action of electromagnetic forces. The constant of electromagnetic interaction is small, and the electromagnetic field decreases more slowly; in addition, in the accelerator vacuum there

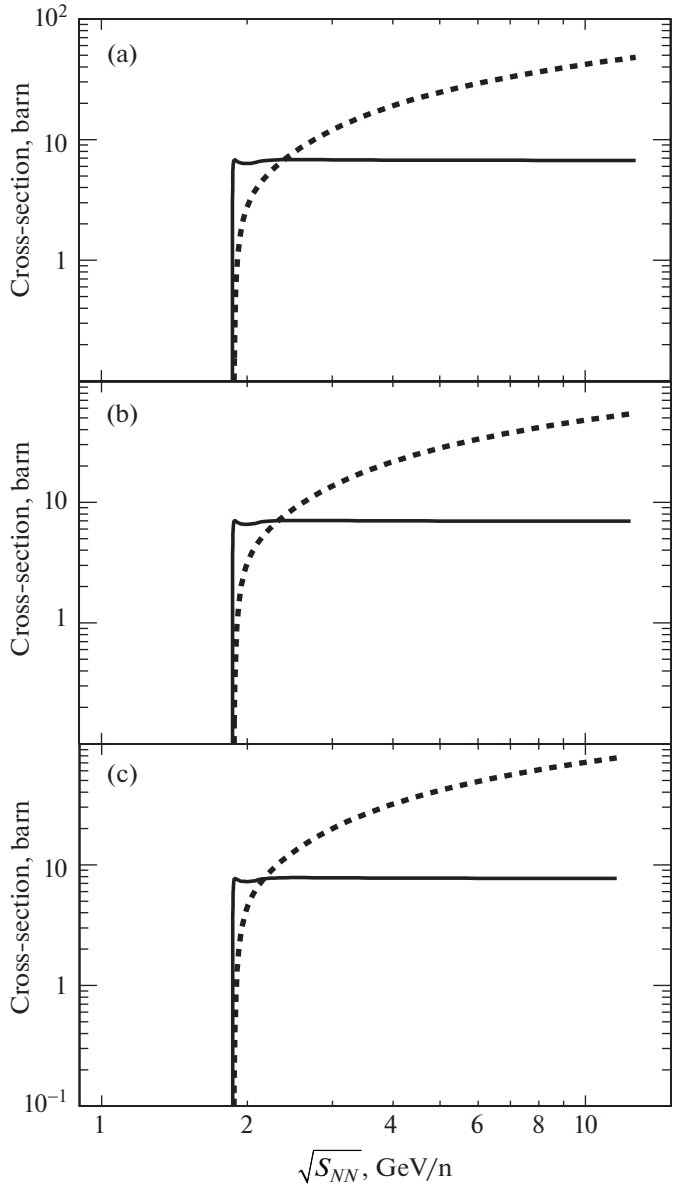

Fig. 2. Calculated dependences of the inelastic collision cross sections of (a) gold, (b) lead, and (c) uranium nuclei on the center-of-mass energy per nucleon. The solid and dashed curves show the inelastic hadronic integral cross section according to the Glauber–Gribov model and the total electromagnetic dissociation cross section, respectively.

is practically no limitation on the growth of the electromagnetic cross section, which is characteristic of shielding by matter. The general observation is that electromagnetic interactions generally dominate over hadronic ones when a relativistic charged particle passes through matter. Moreover, this effect does not depend on the accelerator facility, but is determined only by the energy and atomic number of the colliding nuclei. This means that in the final state, nucleons (and light fragments) and nuclei of the residue will be observed, and the hadronic inelastic cross section (its quasi-elastic part) with the same signature of the final state will be a background process. This is the main conclusion of this work.

Note that relations (8) and (13) describe only the production of nucleons. An extension of the electromagnetic dissociation model of the Geant4 software package to the production of hydrogen isotopes, helium, and other light fragments is under development.

ACKNOWLEDGMENTS

The authors are grateful to A. Ribon (CERN) for useful discussions.

FUNDING

The work was supported by a grant from the Government of the Russian Federation (Agreement No. 075-15-2024-667 dated August, 23 2024)

CONFLICT OF INTEREST

The authors of this work declare that they have no conflicts of interest.

REFERENCES

1. Agapov, N.N., Kekelidze, V.D., Kovalenko, A.D., Lednitsky, R., Matveev, V.A., Meshkov, I.N., Nikitin, V.A., Potrebennikov, Yu.K., Sorin, A.S., and Trubnikov, G.V., Relativistic nuclear physics at JINR: from the synchrophasotron to the NICA collider, *Phys. Usp.,* 2016, vol. 59, no. 4, pp. 383–402. https://doi.org/10.3367/UFNe.0186.201604c.0405

2. Agostinelli, S., Allison, J., Amako, K., et al., Geant4—a simulation toolkit, *Nucl. Instr. Meth. Phys. Res. A,* 2003, vol. 506, pp. 250–303. https://doi.org/10.1016/S0168-9002(03)01368-8

3. Allison, J., Amako, K., Apostolakis, J., et al., Geant4 developments and applications, IEEE Trans. Nucl. Sci., 2006, vol. 53, no. 1, pp. 270–278. https://doi.org/10.1109/TNS.2006.869826

4. Allison, J., Amako, K., Apostolakis, J., et al., Recent developments in GEANT4, *Nucl. Instr. Meth. Phys. Res. A,* 2016, vol. 835, pp. 186–225. https://doi.org/10.1016/j.nima.2016.06.125

5. Bagulya, A.V., Grichine, V.M., Zavestovskaya, I.N., and Ryabov, V.A., Geant4 simulation of the $p + {}^{11}B \to 3\alpha$ reaction, *Bull. Lebedev Phys. Inst.,* 2023, vol. 50, no. 4, pp. 138–143. https://doi.org/10.3103/S1068335623040036

6. Bagulya, A.V., Grichine, V.M., Ryabov, V.A., and Zavestovskaya, I.N., Simulation of Bragg curves produced by protons, alpha-particles, and carbon ions in water, *Bull. Lebedev Phys. Inst.,* 2024, vol. 51, no. 8, pp. 300–305. https://doi.org/10.3103/S1068335624601006

7. Grichine, V.M., A simplified Glauber model for hadron-nucleus cross sections, *Eur. Phys. J. C,* 2009, vol. 62, pp. 399–404. https://doi.org/10.1140/epjc/s10052-009-1033-z

8. Grichine, V.M., A simple model for integral hadron-nucleus and nucleus-nucleus cross-sections, *Nucl. Instr. Meth. B,* 2009, vol. 267, pp. 2460–2462. https://doi.org/10.1016/j.nimb.2009.05.020

9. Geant4 Homepage. Physics Reference Manual. https://geant4-userdoc.web.cern.ch/UsersGuides/PhysicsReferenceManual/html/index.html.

10. Acharya, S., Adamová, D., Adler, A., et al. (ALICE Collaboration), ALICE luminosity determination for Pb–Pb collisions at $\sqrt{s_{\mathrm{NN}}} = 5.02$ TeV, *JINST,* 2024, vol. 19, P02039. https://doi.org/10.1088/1748-0221/19/02/P02039

11. Wilson, J.W., Tripathi, R.K., Cucinotta, F.A., et al., NUCFRG2: An evaluation of the semiempirical nuclear fragmentation database, *NASA Technical Paper 3533,* 1995. https://ntrs.nasa.gov/api/citations/19960003438.

12. Bertulani, C.A., and Baur, G., Electromagnetic processes in relativistic heavy ion collisions, *Nucl. Phys. A,* 1986, vol. 458, pp. 725–744. https://doi.org/10.1016/0375-9474(86)90197-1

Translated by I. Ulitkin